TECHNICAL RESEARCH REPORT

SYSTEMS RESEARCH CENTER

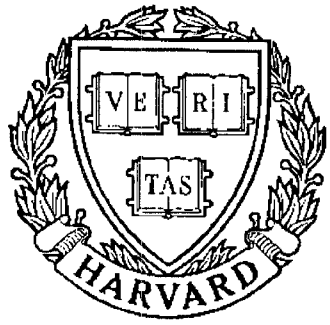

Supported by the National Science Foundation Engineering Research Center Program (NSFD CD 8803012), Industry and the University

On the Contraction Mapping Method for Frequency Detection

by B. Kedem and S. Yakowitz

TR 92-45

On the Contraction Mapping Method for Frequency Detection

Benjamin Kedem[1] and Sidney Yakowitz[2]

[1]Department of Mathematics and Systems Research Center
University of Maryland
College Park, Maryland 20742
and
[2]Systems and Industrial Engineering Department
University of Arizona
Tucson, Arizona 85721

June 1991 [1]

[1]Work supported by grants AFOSR-89-0049 ONR-89-J-1051, and NSF CDR-88-03012.

Abstract

The contraction mapping method for frequency estimation in the presence of noise, identifies the cosine of the frequency to be detected as a fixed point of a certain correlation mapping. At its heart, the method provides a plan for automatic self tuning of parametric filters. A variant of the method, called the HK algorithm, produces recursive zero-crossing rates (normalized HOC sequences) that converge to the frequency of interest. A statistical explanation for the contraction mapping method as epitomized by the HK algorithm is provided when the HOC sequences are produced by bandpass filters. The outright consistency of the zero-crossing rate is not required. Examples show that the method performs quite remarkably.

Abbreviated Title: "Contraction Mappings"

Key words and phrases: Stationary, Gaussian, bandwidth, fixed point, parametric filter, convergence.

AMS subject classification: Primary $62M10$, secondary $62M07$.

1 Introduction

The iterative method for frequency detection discussed in He and Kedem (1989) (HK), Yakowitz (1990) (Y), and Kedem and Yakowitz (1990) (KY), locates discrete frequencies by iterations of a certain contraction mapping. If ω_1 is a frequency to be detected, then $\cos(\omega_1)$ is a fixed point of the mapping, and the method produces a recursive sequence that converges to the fixed point. Thus, the essence of the method is the location of fixed points by recursive sequences. In general, we refer to this method as the *contraction mapping* (CM) method . A specific special case is the algorithm suggested in HK. It makes use of the zero-crossing rate observed in filtered time series.

Suppose $\{\mathcal{L}_r, r \in (-1,1)\}$ is a parametric family of time invariant linear filters defined from a real valued impulse response sequence $h(n;r)$, $n = 0, \pm 1, \cdots$, which satisfies a certain requirement about r. The HK algorithm is given in terms of the recursion

$$r_{k+1} = \cos(\gamma_{r_k})$$

where γ_r is the observed asymptotic zero-crossing rate after the application of $\{\mathcal{L}_r\}$. γ_r is an example of observed (normalized) higher order crossings (HOC). If ω_1 is the frequency to be detected, then under appropriate conditions, r_k converges to $\cos(\omega_1)$, so that γ_{r_k} converges to ω_1, as $k \to \infty$. Looked at from a more general point of view, the HK algorithm provides a *sequence of self-tuned filters whose successive application yields a sequence of convergent zero-crossing rates.*

In this paper we discuss the strong consistency of the HK algorithm, and illustrate its use through some examples. In particular, in Example 6, the algorithm is applied in the search of a diurnal cycle in a well known precipitation data set. Our analysis supports the hypothesis that tropical rainfall contains a diurnal cycle.

After a short introduction to the CM method in section 2, we illustrate the method in section 3 by appealing to two useful families of bandpass filters. Section 4 discusses the statistical basis for the CM method as epitomized by the HK algorithm, when a family of *bandpass* filters is used in generating convergent (normalized) HOC sequences. The main result is Theorem 4.1, formulated for the bandpass case. Basically it says that if the bandwidth is made to shrink at a certain rate, $\gamma_{r_k} \to \omega_1$ with probability one.

Our approach does not require an outright consistency of the zero-crossing rate. Successive narrowing of the bandwidth renders the zero-crossing rate more and more accurate.

Experimental results in section 4, using a particularly convenient family of bandpass filters, confirm what is suggested by the statistical analysis, namely, the convergence of the observed (normalized) HOC sequences toward the desired frequency is rather fast and precise as the bandpass is squeezed in a controlled manner. The examples show that the CM method can provide more precise estimates than does periodogram analysis.

1.1 Definition of HOC

Let $\{Z_t\}$, $t = 0, \pm 1, \pm 2, \cdots$, be a real valued zero-mean stationary time series, and let $\{\mathcal{L}_\theta\}$, $\theta \in \Theta$, be a parametric family of time invariant linear filters. Denote by $\{Z_t(\theta)\}$ the filtered series,

$$Z_t(\theta) = \mathcal{L}_\theta(Z)_t$$

Let $I_{[\mathcal{A}]}$ be the indicator of the event $\mathcal{A}$, and suppose $\{Z_t(\theta)\}$ is a real valued process. The quantity

$$D_\theta \equiv \sum_{t=2}^{N} I_{[Z_t(\theta)Z_{t-1}(\theta)<0]}$$

gives the number of zero-crossings (in discrete time) observed in

$$Z_1(\theta), Z_2(\theta), \cdots, Z_N(\theta)$$

The family $\{D_\theta\}, \theta \in \Theta$ is called a (observed) *higher order crossings* family, or HOC. The corresponding expected HOC family is given by $\{E(D_\theta)\}, \theta \in \Theta$.

The sample zero-crossing rate is defined from the normalized HOC,

$$\hat{\gamma}_\theta = \frac{\pi D_\theta}{N-1} \tag{1}$$

When $\{Z_t\}$ is strictly stationary, the asymptotic zero-crossing rate is defined by the almost sure limit of the sample zero-crossing rate,

$$\gamma_\theta \equiv \lim_{N\to\infty} \hat{\gamma}_\theta = \lim_{N\to\infty} \frac{\pi D_\theta}{N-1} \tag{2}$$

Note that $E(\hat{\gamma}_\theta) = E(\gamma_\theta)$

2 The CM method

We shall adhere to the mixed spectrum model

$$Z_t = A_1 \cos(\omega_1 t) + B_1 \sin(\omega_1 t) + \zeta_t \tag{3}$$

where, $t = 0, \pm 1, \pm 2, \cdots$, A_1 and B_1 are uncorrelated normal random variables with $E(A_1) = E(B_1) = 0$, and $Var(A_1) = Var(B_1) = \sigma_1^2$. Further, suppose $\{\zeta_t\}$ is colored stationary Gaussian noise with mean 0 and variance σ_ζ^2, independent of the A_1 and B_1. The noise is assumed to possess an absolutely continuous spectral distribution function $F_\zeta(\omega)$ with spectral density $f_\zeta(\omega)$, $\omega \in [-\pi, \pi]$.

Let r be a parameter that takes values in $(-1, 1)$, and consider the parametric family of linear filters $\{\mathcal{L}_r\}$ defined by the family of impulse response sequences $\{h(n; r)\}$, $n = 0, \pm 1, \cdots$. The corresponding family of transfer functions is denoted by $\{H(\omega; r)\}$, $\omega \in [-\pi, \pi]$. Let $Z_t(r)$ and $\zeta_t(r)$, $t = 0, \pm 1, \cdots$, be the filtered process and filtered noise, respectively. The essential element of the CM method is the assumption that the real part of *the first-order autocorrelation of the filtered noise* $\zeta_t(r)$ *is* r. In symbols, we assume that (HK,Y),

$$r = \Re \left\{ \frac{E[\zeta_t(r)\overline{\zeta_{t-1}(r)}]}{E|\zeta_t(r)|^2} \right\}$$

where the overbar denotes complex conjugate. This means that we require the *fundamental property*,

$$r = \frac{\int_{-\pi}^{\pi} \cos(\omega) |H(\omega; r)|^2 f_\zeta(\omega) d\omega}{\int_{-\pi}^{\pi} |H(\omega; r)|^2 f_\zeta(\omega) d\omega} \tag{4}$$

The fundamental property (4) is exhibited by many filters of which the $AR(1)$ filter (also known as exponential smoothing)

$$\mathcal{L}_\alpha \equiv 1 + \alpha \mathcal{B} + \alpha^2 \mathcal{B}^2 + \cdots, \alpha \in (-1, 1) \tag{5}$$

where $\mathcal{B}$ is the backward shift, is the clearest example when used in conjunction with white noise ζ_t (see HK).

Let $\rho_1(r)$ be the real part of the first order autocorrelation of $\{Z_t(r)\}$,

$$\rho_1(r) = \Re \left\{ \frac{E[Z_t(r)\overline{Z_{t-1}(r)}]}{E|Z_t(r)|^2} \right\}$$

and assume that $\mathcal{L}_r$ "passes ω_1". That is, $|H(\omega;r)|$ is positive in a neighborhood of ω_1 for some r. Then (4) implies that (HK, Y),

$$\rho_1(r) = \frac{\frac{1}{2}\sigma_1^2[|H(-\omega_1;r)|^2 + |H(\omega_1;r)|^2]\cos(\omega_1) + \left[\int_{-\pi}^{\pi} |H(\omega_1;r)|^2 dF_\zeta(\omega)\right] r}{\frac{1}{2}\sigma_1^2[|H(-\omega_1;r)|^2 + |H(\omega_1;r)|^2] + \int_{-\pi}^{\pi} |H(\omega_1;r)|^2 dF_\zeta(\omega)} \quad (6)$$

This function of r is a weighted average of $\cos(\omega_1)$ and r. It admits the more compact representation,

$$\rho_1(r) = r^* + C(r)(r - r^*) \quad (7)$$

where $r^* = \cos(\omega_1)$, and

$$C(r) = \frac{E|\zeta_t(r)|^2}{E|Z_t(r)|^2} \quad (8)$$

Clearly $0 \leq C(r) \leq 1$, and $C(r) = 1$ when the filter does not pass ω_1. When $C(r) < 1$ in a neighborhood of r^*, we identify the mapping (7) as a contraction at r^* with a contraction factor $C(r)$. From the recursion

$$r_{k+1} = \rho_1(r_k) \quad (9)$$

we obtain

$$\rho_1(r_k) = r^* + [\prod_{j=1}^{k} C(r_j)](r - r^*)$$

If $\prod_{j=1}^{k} C(r_j) \to 0$, then

$$r_k \to r^* \quad (10)$$

and

$$\cos^{-1}(r_k) \to \omega_1$$

as $k \to \infty$. We now summarize the preceding discussion in

Theorem 2.1 *Let $\{Z_t\}$ be given by (3), and let $\{\mathcal{L}_r\}$ be a parametric family of time invariant linear filters for which the fundamental property (4) holds, and one that passes ω_1. Let $\rho_1(r)$ be the real part of the first-order autocorrelation of the filtered process $Z_t(r) \equiv \mathcal{L}_r(Z)_t$. Fix $r_0 \in (-1,1)$. If $\prod_{j=1}^{k} C(r_j) \to 0$, then r_k, defined by the recursion $r_{k+1} = \rho_1(r_k)$, converges to $\cos(\omega_1)$, and*

$$\cos^{-1}(r_k) \to \omega_1$$

as $k \to \infty$.

The recursion (9) characterizes the CM method. It suggests the procedure

$$r_{k+1} = \hat{\rho}_1(r_k) \tag{11}$$

where $\hat{\rho}_1(r)$ is a suitable estimator of $\rho_1(r)$ from a time series $Z_1, \cdots, Z_N$, of size N.

In the real Gaussian case, a natural estimator is obtained from the "cosine formula" (see the discussion in Barnett and Kedem (1991))

$$\rho_1(r) = \cos(E(\gamma_r))$$

and the algorithm takes the specific form (HK)

$$r_{k+1} = \cos(\gamma_{r_k}) \tag{12}$$

where γ_{r_k} is the observed asymptotic zero-crossing rate as defined in (2). We can now see that the HK algorithm (12) is a special case of the CM method.

In the Gaussian case there is a certain advantage for using an estimate from zero-crossings. In the mixed spectrum case, the sample autocorrelation is not necessarily a consistent estimator. Likewise, the sample zero-crossing rate is in general not a consistent estimator for its expectation when the spectrum contains jumps. However, the asymptotic zero-crossing rate falls with probability one between the lowest and highest nonnegative frequencies in the spectral support, so that its variability can be controlled by the application of bandpass filters. See Kedem and Slud (1991) (KS) for a detailed discussion regarding the consistency of the sample autocorrelation and the sample zero-crossing rate.

In the real nonGaussian case, when the HOC family is obtained from bandpass filters with narrow bandwidth, the cosine formula provides an excellent approximation to the first order autocorrelation, and the HK algorithm (12) performs remarkably well. Evidence of this is given in Examples 2 and 6 below.

3 Two parametric families of filters

This section discusses the CM plan relative to two useful parametric bandpass filters. In addition, it is shown that the contraction factor can in fact be controlled by the filter bandwidth.

3.1 The complex exponential filter

A useful example (Y,KY), that illustrates the contraction mapping algorithm (9) and its key elements, is provided in terms of a parametric family of linear filters defined by the impulse response

$$h(n;r,M) = \begin{cases} \exp(in\theta(r))/\sqrt{2M+1}, & |n| \leq M \\ 0, & |n| > M \end{cases} \tag{13}$$

where $\theta(r) = \cos^{-1}(\frac{2M+1}{2M}r) \approx \cos^{-1}(r)$. Because of the particular form of this impulse response, we shall refer to this filter as the "complex exponential filter". The corresponding squared gain is

$$|H(\omega;r,M)|^2 = \frac{1}{2M+1}\frac{\sin^2[\frac{1}{2}(2M+1)(\omega-\theta(r))]}{\sin^2[\frac{1}{2}(\omega-\theta(r))]}, \quad -\pi \leq \omega \leq \pi \tag{14}$$

which we recognize as the Fejer kernel centered at $\theta(r)$. This parametric family also motivates a certain assumption concerning the contraction factor needed for the proof of our main result in the next section.

One can see that $|H(\omega;r,M)|^2$ assumes its maximum value, which is $2M+1$, at $\omega = \theta(r)$. This filter is essentially a bandpass filter centered at $\theta(r)$, and its dominant lobe is supported over the interval

$$\mathcal{I} = (\theta(r) - 2\pi/(2M+1), \theta(r) + 2\pi/(2M+1))$$

For sufficiently large M, we can think of I as the effective bandwidth of the filter. The complex case follows the footsteps of the real case except that now we use the real part of the concerned autocorrelations. Thus, *under the assumption of white noise*, the fundamental property (4) now takes the form

$$r = \Re\left\{\frac{E[\zeta_t(r,M)\overline{\zeta_{t-1}(r,M)}]}{E|\zeta_t(r,M)|^2}\right\} \tag{15}$$

where $\zeta_t(r,M)$ is the filtered noise (it is not white anymore). It is easy to check that (15) holds for $|r| \leq 2M/(2M+1)$. Similarly, the correlation mapping is now defined by

$$\rho_1(r) = \Re\left\{\frac{E[Z_t(r,M)\overline{Z_{t-1}(r,M)}]}{E|Z_t(r,M)|^2}\right\}$$

where $Z_t(r, M)$ is the filtered process, and the dependence of $\rho_1(r)$ on M is suppressed for notational convenience. Thus defined, $\rho_1(r) = \rho_1(r, M)$ satisfies

$$\rho_1(r) - r^* = \frac{E|\zeta_t(r, M)|^2}{E|Z_t(r, M)|^2}(r - r^*) \equiv C(r)(r - r^*) \tag{16}$$

which is a contraction mapping at $r^* = \cos(\omega_1)$, as long as ω_1 passes, with contraction factor (in the present complex case the gain is not symmetric; when M is sufficiently large negative frequencies and in particular $-\omega_1$ are suppressed)

$$C(r) \doteq \frac{\sigma_\zeta^2}{\frac{\sigma_1^2}{2}|H(\omega_1; r, M)|^2 + \sigma_\zeta^2} \tag{17}$$

where again, the dependence of $C(r)$ on M is suppressed for notational convenience. The recursion $r_{k+1} = \rho_1(r_k)$ yields the convergence $r_k \to r^*$, provided $\Pi_{j=1}^k C(r_j) \to 0$, as $k \to \infty$.

3.1.1 Bounding the contraction factor by the bandwidth

As is clear from the preceding paragraph, enhanced speed of convergence towards r^* can be obtained by decreasing the contraction factor $C(r_j)$ with each iteration of the CM recursion (KY). This, however, can be achieved by controlling the effective bandwidth of the filter. The following result, which helps in motivating a certain assumption, renders this idea more precise.

Proposition 3.1 *Under the assumption of white noise, let* $|H(\omega_1; r, M)|^2$ *be as in (14), and assume,*

$$\omega_1 \in [\omega_a, \omega_b] \subset \mathcal{I}$$

Define

$$\Delta \equiv \omega_b - \omega_a$$

Then there exists a $\overline{C}(M)$*, which does not depend on* r*, satisfying*

$$0 < C(r) \leq \overline{C}(M) < 1$$

and $\overline{C}(M)$ *is of order* $O(\Delta)$ *as* $\Delta \to 0$.

Proof: By centering the filter at 0,

$$|H(\omega_1; r, M)|^2 = |H(\omega_1 - \theta(r); \frac{2M}{2M+1}, M)|^2$$

Therefore, when $\omega_1, \theta(r) \in [\omega_a, \omega_b]$,

$$|H(\Delta; \frac{2M}{2M+1}, M)|^2 < |H(\omega_1 - \theta(r); \frac{2M}{2M+1}, M)|^2$$

Define

$$\overline{C}(M) = \frac{\sigma_\zeta^2}{\frac{\sigma_1^2}{2}|H(\Delta; \frac{2M}{2M+1}, M)|^2 + \sigma_\zeta^2} \tag{18}$$

Then in light of (17),

$$0 < C(r) \leq \overline{C}(M) < 1$$

As $\Delta \to 0$, choose $M = O(1/\Delta)$. □

As a matter of fact, by minimizing (18) with respect to M, the optimal value of M is approximately $1.165/\Delta$.

Proposition 2.1 can be demonstrated graphically as well. Figure 1 (a) shows the graph of $\rho_1(r, 20)$ when $\omega_1 = 0.8$ radians per unit time, and $\sigma_1^2 = \sigma_\zeta^2 = 1$. In a neighborhood of $r^* = \cos(0.8) = 0.697$, we can see from the figure that the derivative $\rho_1'(r, 20)$ is very close to 0, and this is already with $M = 20$. Therefore, in a neighborhood of r^*,

$$0 \approx \rho_1'(r^*, 20) \approx \frac{\rho_1(r, 20) - r^*}{r - r^*} = C(r, 20)$$

However, the effective bandwidth of the filter in a neighborhood of $\theta = 0.8$ is considerably greater than 0, as can be seen from Figure 1 (b).

3.2 A complex filter

He and Kedem (1989) considered the parametric filter defined by,

$$Z_t(r; M) = \left(1 + e^{i\theta(r)}\mathcal{B}\right)^M Z_t$$

where M is a positive integer, $r \in (-1,1)$, and $\theta(r) \in (-\pi,\pi)$. For sufficiently large M, for example $M = 30$, this filter acts as a bandpass filter with impulse response and squared gain given by, respectively,

$$h(n;r,M) = \begin{cases} \binom{M}{n} e^{i\theta(r)n}, & n = 0,\cdots,M \\ 0, & \text{otherwise} \end{cases} \tag{19}$$

and,

$$|H(\omega;r,M)|^2 = 4^M \cos^{2M}\left(\frac{\omega-\theta(r)}{2}\right) \tag{20}$$

The fundamental property is obtained by *defining*,

$$r = \frac{\int_{-\pi}^{\pi} \cos^{2M}\left(\frac{\lambda-\theta(r)}{2}\right)\cos(\lambda)dF_\zeta(\lambda)}{\int_{-\pi}^{\pi} \cos^{2M}\left(\frac{\lambda-\theta(r)}{2}\right)dF_\zeta(\lambda)} \tag{21}$$

When $\{\zeta_t\}$ is white noise (HK),

$$r \to \cos(\theta(r)),\ M \to \infty$$

and we have the approximation $\theta(r) \approx \cos^{-1}(r)$. As in the previous case, it is easy to see that this approximation holds true for any continuous spectrum noise, provided the spectral density is sufficiently smooth. For sufficiently large M, e.g. $M = 100$, when the filter is centered at $\theta(r)$ near ω_1, it only passes a band of frequencies in a neighborhood of ω_1 (see Figure 2 (b)) and we obtain from (21) the mapping,

$$\rho_1(r) = \cos(\omega_1) + C(r)(r - \cos(\omega_1))$$

with

$$C(r) = \frac{E|\zeta_t(r)|^2}{\frac{\sigma_1^2}{2}|H(\omega_1;r,M)|^2 + E|\zeta_t(r)|^2}$$

In Kedem and Lopes (1991) it is shown that there exists an increasing sequence $\{M_k\}$ such that

$$r_{k+1} = \rho_1(r_k, M_k) \to \cos(\omega_1), \quad k \to \infty$$

Figure 2 (a) shows the graph of $\rho_1(r) = \rho_1(r, 100)$, for $M = 100$, $\omega = 0.8$, and $\sigma_1^2 = \sigma_\zeta^2 = 1$. As with the complex exponential filter, the derivative of $\rho_1(r, 100)$ near $\cos(0.8)$ is close to 0, so that $C(r) = C(r, 100)$ is rather small, *much smaller than the bandwidth* given in Figure 2 (b), and we can see that $\rho_1(r)$ is a contraction at $r^* = \cos(\omega_1) = \cos(0.8)$. Furthermore, the figure gives additional evidence that the contraction factor can be bounded by the bandwidth in a neighborhood of r^*.

Remark 3.2.1 In the multiple frequency case, it was proved in HK that in the purely discrete spectrum case ($\sigma_\zeta^2 = 0$), for *fixed* θ, $\rho_1(\theta)$ (obvious notation) converges to the frequency closest to θ, as $M \to \infty$. However, when white noise is present, the convergence is toward $\cos(\theta)$. In other words, by shrinking the bandwidth without "sliding the filter", the frequency closest to the center of the frequency is lost. The frequency, however, is not lost if we decrease the bandwidth and slide the gain toward the frequency at the same time. This is the essence of the CM method.

4 Convergence in the bandpass case

Suppose the parametric family $\{\mathcal{L}_r\}$ defines a family of bandpass filters satisfying (4), where $\mathcal{L}_r$ has bandwidth of size W_r stretching from ${}_*\omega$ to ω^*, $[{}_*\omega, \omega^*] \subset [0, \pi]$. Let $\{D_r\}$ be the corresponding HOC family obtained from a time series of length N. Consider the asymptotic zero-crossing rate,

$$\gamma_r \equiv \lim_{N\to\infty} \hat{\gamma}_r = \lim_{N\to\infty} \frac{\pi D_r}{N-1}$$

From (KS) we know that γ_r is most likely a random variable (mixed spectrum in a Gaussian process), but that it (and hence also its expected value) falls in the bandpass with probability one. Thus, by controlling W_r, we can control the variability of γ_r, and make it arbitrarily small. Because this fact is of vital importance in the following development, we state it formally.

Proposition 4.1 *(KS). Assume that the real-valued, stationary, zero-mean Gaussian process* $\{Z_t\}$ *has normalized spectral measure* ν *supported on* $\mathbf{J} \cup (-\mathbf{J})$ *where*

$$\mathbf{J} = [{}_*\omega, \omega^*] \subset [0, \pi]$$

Then, whether ν has atoms or not, the asymptotic zero-crossing rate γ_r lies in **J** *with probability one.*

Thus, γ_r falls with probability one between the lowest ($_*\omega$) and highest (ω^*) nonnegative frequencies. As a consequence also $E(\gamma_r)$ falls in $[_*\omega, \omega^*]$, and we have the following fact.

Corollary 4.1 *Let a be any number between γ_r and $E(\gamma_r)$, and let W_r be the length (bandwidth) of the interval $[_*\omega, \omega^*]$. Then*

$$|\gamma_r - E(\gamma_r)||\sin(a)| \leq W_r$$

with probability one.

The purpose of the corollary is to motivate Assumption **A2** below.

The Gaussian assumption and the contraction mapping (7) give

$$\rho_1(r) = \cos(E(\gamma_r)) = r^* + C(r)(r - r^*)$$

where now $C(r)$ depends on the bandwidth parameter W_r. The Mean Value Theorem implies

$$\cos(\gamma_r) - \cos(E(\gamma_r)) = -(\gamma_r - E(\gamma_r))\sin(z_r)$$

where z_r is between γ_r and $E(\gamma_r)$. If we define $y_r \equiv -(\gamma_r - E(\gamma_r))\sin(z_r)$, then we obtain the *observed contraction mapping*

$$\cos(\gamma_r) = r^* + C(r)(r - r^*) + y_r \tag{22}$$

This expression identifies the exact error incurred by replacing $\cos(E(\gamma_r))$ by $\cos(\gamma_r)$. Now consider the HK algorithm

$$r_{k+1} = \cos(\gamma_{r_k}) \tag{23}$$

This and (22) give

$$r_{k+1} = r^* + [\prod_{j=1}^{r_k} C(r_j)](r_1 - r^*) + [\prod_{j=2}^{r_k} C(r_j)]y_{r_1} + \cdots + C(r_k)y_{r_{k-1}} + y_{r_k} \tag{24}$$

To achieve convergence, the bandwidth must go to 0 at a certain rate. To uncover this rate, we resort to the following assumptions.

A1. Motivated by Proposition 3.1 and Figures 1,2, we assume that in a neighborhood of r^*, $C(r_k)$ is smaller than the bandwidth times a constant. Formally we assume that there is a positive constant K such that

$$0 < C(r_k) < KW_k$$

A2. Motivated by Corollary 4.1, we assume that

$$|y_{r_k}| < KW_k$$

where, for simplicity, K is as in **A1.**.

Remark 4.1. Figures 1,2, indicate that there are cases where $C(r_k)$ is very close to 0 in a neighborhood of r^* in addition to being much smaller than the bandwidth. Thus, A1 is very plausible. Note however, that we stress the requirement of being in a neighborhood of r^*, for otherwise, when the frequency "is not captured," $C(r_k)$ is equal to 1 (case of ideal bandpass) and convergence toward the frequency does not occur.

Remark 4.2. In light of Corollary 4.1, A2 is very plausible also. However, it should be noted that in Corollary 4.1, the parameter r is fixed, while it is random in A2.

So, under these assumptions,

$$|r_{k+1} - r^*| \leq KW_k \{1 + KW_{k-1} + \cdots + (KW_2 \cdots KW_{k-1})\} + \left\{ \prod_{j=1}^{k} KW_j \right\} (r_1 - r^* + 1) \qquad (25)$$

We can now shrink the bandwidth W_k, as $k \to \infty$, at a rate (for example at a rate of $1/k$) that guarantees the almost sure convergence of r_k to r^*. In this case,

$$\gamma_{r_k} \to \omega_1$$

almost surely. In summary we have.

Theorem 4.1 *Let $\{Z_t\}$ be given by (3), and let $\{\mathcal{L}_r\}$, $r \in (-1,1)$, be a parametric family of time invariant bandpass linear filters, with bandwidth W_r, for which the fundamental property (4) holds, and one that passes ω_1. Assume that the filtered process $\{Z_t(r)\}$ is real valued for all $r \in (-1,1)$. Consider the recursion*

$$r_{k+1} = \cos(\gamma_{r_k})$$

and suppose W_{r_k} is of the order $O(1/k)$. If A1 and A2 hold, then

$$\gamma_{r_k} \rightarrow \omega_1 \tag{26}$$

with probability one.

4.1 Connection between C(r) and the SNR

The signal to noise ratio (SNR) for the process (3) is defined by

$$SNR = 20 \log_{10} \frac{\sigma_1}{\sigma_\zeta} dB$$

In general, the SNR is defined by,

$$SNR = 10 \log_{10} \frac{\text{Variance of the filtered signal}}{\text{Variance of the filtered noise}} dB$$

from which it follows that the SNR can be expressed in terms of the contraction factor,

$$SNR = 10 \log_{10} \{ \frac{1}{C(r)} - 1 \} \tag{27}$$

Thus, the SNR and $C(r)$ are inversely related:

$$SNR \rightarrow \infty \iff C(r) \rightarrow 0$$

$$SNR \rightarrow -\infty \iff C(r) \rightarrow 1$$

Because we can control y_r by varying the bandwidth, and in addition in practice y_r is rather small (KS), (27) shows that the speed of convergence of r_k, depends primarily on the contraction factor $C(r)$. The smaller $C(r)$ is, the faster is the speed of convergence.

4.2 Examples

The HK algorithm $r_{k+1} = \cos(\hat{\gamma}_{r_k})$ was applied to time series of length $N = 2000$[1] from the process (3) with Gaussian white noise ζ_t, unless stated otherwise, using the real counterpart of the complex filter (13),

$$h(n; r, M) = \begin{cases} \cos(n\theta(r))/\sqrt{2M+1}, & |n| \leq M \\ 0, & |n| > M \end{cases} \tag{28}$$

We refer to this filter as the "cosine filter". The corresponding squared gain, $|\tilde{H}(\omega; r, M)|^2$, is closely related to $|H(\omega; r, M)|^2$ in (14) for $\omega > 0$,

$$|\tilde{H}(\omega; r, M)|^2 = \frac{1}{4}|H(\omega; r, M)|^2 + O(\frac{1}{M}) \tag{29}$$

Figure 3 shows the graph of $|\tilde{H}(\omega; r, M)|^2$, $\omega > 0$, with $(M_1 = 20, \theta(r_1) = 1)$ and $(M_2 = 40, \theta(r_2) = 1.1)$. The figure illustrates a shift in location accompanied by a reduced bandwidth.

As can be seen from the tables in the following examples, the convergence is very fast, and the frequency is never lost when M_k increases at a linear rate such as $\{5, 15, 25, 35, \cdots\}$. Roughly, this is equivalent to a bandwidth that shrinks at the order of $O(1/k)$. Also note that the sequence of observed zero-crossing rates $\{\hat{\gamma}_{r_k}\}$ is monotone, with a possible exception of the very beginning, as is well expected from (7) and (9).

Very similar results were obtained by a variety of other bandpass filters.

It should be noted that in Y and KY the autocorrelation was estimated from the sample autocorrelation of the filtered processes, while here the estimates are obtained from the observed zero-crossing rate after filtering as suggested from HK and KS. Evidently, the two methods of estimation, in conjunction with the CM method, give very similar frequency estimates for sufficiently long data sets.

[1] More precisely, for a given M_k, the zero-crossing count is computed from time series of length $2000 + 2M_k$.

4.2.1 Example 1: A simple case

$\omega_1 = 0.8$, $\theta(r_0) = 0.4$, $A_1 = -0.91333, B_1 = 0.06975$, $SNR = 0dB$,

k	M_k	r_k	$\hat{\gamma}_{r_k}$
0	5	0.92106	0.65221
1	15	0.79475	0.75279
2	25	0.72979	0.79994
3	35	0.69675	0.79994
4	45	0.69675	0.79994
5	55	0.69675	0.79994
.	.	.	.
.	.	.	.
.	.	.	.
			$\hat{\omega}_1 = 0.79994$

For comparison, the five highest periodogram ordinates, ordered by magnitude, were at the frequencies:

0.80185, 0.80485, 2.26793, 0.74201, 0.83776

with the maximum occurring at 0.80185.

4.2.2 Example 2: NonGaussian and colored noise

When the fundamental property (4) holds for white noise, it also holds approximately for slowly varying continuous spectral densities, as long as the bandwidth is sufficiently narrow. In this respect, it is of interest to apply the HK algorithm with the cosine filter and colored Gaussian noise. It is also interesting to run the algorithm when the noise is white but nonGaussian. Accordingly, we have applied the algorithm when ζ_t is Gaussian white noise (GWN), lognormal white noise (LNWN) (with parameters 0,1 , and properly centered and scaled), and a first-order moving average (MA(1)), $u_t = \zeta_t - 0.8\zeta_{t-1}$, and ζ_t Gaussian white noise. In all three cases the sinusoidal component was identical. The results are given in the following table, and show identical convergence. Evidently, in the bandpass case, the algorithm is quite robust.

$\omega_1 = 0.71$, $\theta(r_0) = 1.1$, $A_1 = -0.954817, B_1 = 1.00687$,
$SNR = 0dB$,

		GWN	LNWN	MA(1)
k	M_k	$\hat{\gamma}_{r_k}$	$\hat{\gamma}_{r_k}$	$\hat{\gamma}_{r_k}$
0	5	0.993240	0.913089	0.997955
1	15	0.920947	0.897373	0.928805
2	25	0.812508	0.766932	0.848654
3	35	0.766932	0.710355	0.748073
4	45	0.719785	0.710355	0.710355
5	55	0.710355	0.710355	0.710355
6	65	0.710355	0.710355	0.710355
.	.	.	.	.
.	.	.	.	.
.	.	.	.	.
		$\hat{\omega}_1 = 0.710355$	$\hat{\omega}_1 = 0.710355$	$\hat{\omega}_1 = 0.710355$

4.2.3 Example 3: Mixed spectrum noise

In this example we compare the convergence of the HK algorithm in two cases when the noise ζ_t is Gaussian white noise, and then when it is Gaussian white noise plus a random Gaussian sinusoid (mixed spectrum noise) with frequency 2.5. In both cases the "signal" is a random Gaussian sinusoid with frequency $\omega_1 = 1.25$, and the search starts at $\theta(r_0) = 0.5$. We have: $A_1 = 0.30041, B_1 = -1.44635$, the amplitude of the sinusoidal noise component is 0.947085, and $SNR = 0dB$. Again, from the table, the convergence is very satisfactory.

This example shows that our algorithm can be applied separately to each frequency using bandpass filters. In fact when $\theta(r_0) = 2.3$ the $\hat{\gamma}_{r_k}$ converges to 2.50039, and the other frequency is detected as expected.

		GWN	Mixed Spectrum Noise
k	M_k	$\hat{\gamma}_{r_k}$	$\hat{\gamma}_{r_k}$
0	5	0.93509	1.09854
1	15	1.05296	1.23684
2	25	1.16140	1.24941
3	35	1.16454	1.24941
4	45	1.22426	1.24941
5	55	1.24941	1.24941
6	65	1.24941	1.24941
7	75	1.24941	1.24941
8	85	1.24941	1.24941
.	.	.	.
.	.	.	.
.	.	.	.
		$\hat{\omega}_1 = 1.24941$	$\hat{\omega}_1 = 1.24941$

With Gaussian white noise, the highest peaks in the periodogram, ordered by magnitude, occur at the frequencies,

$$1.25366, 1.25068, 1.18815, 1.09286, 1.30726$$

with the highest peak occurring at 1.25366. This is the periodogram estimate.

4.2.4 Example 4: Moderately low SNR

$\omega_1 = 0.4, \theta(r_0) = 0.2, A_1 = -0.537689, B_1 = -0.423486, SNR = -6.0206dB,$

k	M_k	r_k	$\hat{\gamma}_{r_k}$
0	5	0.98007	0.33160
1	15	0.94552	0.40075
2	25	0.92077	0.40075
3	35	0.92077	0.40075
4	45	0.92077	0.40075
5	55	0.92077	0.40075
.	.	.	.
.	.	.	.
.	.	.	.
			$\hat{\omega}_1 = 0.40075$

The highest periodogram ordinates correspond to the frequencies

$$0.40392, 1.93283, 0.46376, 2.01660, 2.05550$$

The largest peak occurs at 0.40392.

4.2.5 Example 5: low SNR

$\omega_1 = 1.95, \theta(r_0) = 1.8, A_1 = 0.174937, B_1 = -0.263656, SNR = -13.9794dB.$

k	M_k	r_k	$\hat{\gamma}_{r_k}$
0	5	-0.22720	1.87647
1	15	-0.30094	1.89690
2	25	-0.32035	1.91576
3	35	-0.33816	1.93776
4	45	-0.35878	1.95191
5	55	-0.37195	1.94876
6	65	-0.36903	1.94876
7	75	-0.36903	1.94876
8	85	-0.36903	1.94876
.	.	.	.
.	.	.	.
.	.	.	.
			$\hat{\omega}_1 = 1.94876$

The five highest peaks in the periodogram are at

$$2.18584, 2.36873, 1.27729, 0.51327, 1.02655$$

where the highest power is given to 2.18584.

4.2.6 Example 6: Detection of a diurnal cycle

GATE stands for GARP (Global Atmospheric Research Program) Atlantic Tropical Experiment (see Simpson (1988)). The experiment, conducted in 1974 in the eastern Atlantic off the coast of west Africa, produced large snapshots of instantaneous tropical rain rate collected in 15 minutes intervals. The experiment was conducted in stages of which the first is referred to as GATE I. The hourly GATE I data[2], averaged over a region of 280×280 km^2, are plotted in Figure 4.

[2]Thanks are due to Dr. Tom Bell, NASA, Goddard SFC, for kindly supplying the hourly GATE data.

From an atmospheric dynamics point of view, it is useful to know whether tropical rainfall contains a significant diurnal cycle (Simpson (1988), p. 40). It is believed that the GATE I data set does contain a significant diurnal cycle. However, so far, the detection of the diurnal cycle in GATE has not been quite decisive.

We have applied the HK algorithm, using the cosine filter, to the centered hourly GATE I data in search of a diurnal cycle. As can be seen from the following table, starting from various points, the convergence is toward the value 0.262675 radians per hour. This gives a period of

$$\frac{2\pi}{0.262675} = 23.92 \text{ hours}$$

which gives more credence to the the existence of a diurnal cycle in GATE I.

		$\theta(r_0) = 0.50$	$\theta(r_0) = 0.45$	$\theta(r_0) = 0.30$
k	M_k	$\hat{\gamma}_{r_k}$	$\hat{\gamma}_{r_k}$	$\hat{\gamma}_{r_k}$
0	55	0.483322	0.441294	0.273182
1	56	0.420280	0.441294	0.262675
2	57	0.367745	0.399266	0.262675
3	58	0.346731	0.346731	0.262675
4	59	0.304703	0.304703	0.262675
5	60	0.294196	0.294196	0.262675
6	61	0.283689	0.283689	0.262675
7	62	0.262675	0.262675	0.262675
8	63	0.262675	0.262675	0.262675
9	64	0.262675	0.262675	0.262675
.	.	.	.	.
.	.	.	.	.
.	.	.	.	.
		$\hat{\omega}_1 = 0.262675$	$\hat{\omega}_1 = 0.262675$	$\hat{\omega}_1 = 0.262675$

4.2.7 Example 7: Comparison between two filters

The real counterpart of the complex filter defined by (19) is obtained from the real impulse response,

$$h(n;r,M) = \begin{cases} \begin{pmatrix} M \\ n \end{pmatrix} \cos(\theta(r)n), & n = 0, \cdots, M \\ 0, & \text{otherwise} \end{cases} \tag{30}$$

We refer to this filter as the "cosine-binomial" filter. To achieve a degree of precision comparable to the one achieved by the cosine filter (28), usually a larger M is needed for the cosine-binomial filter (30).

The following table compares the performance of the cosine filter with that of the cosine-binomial filter considering only six iterations of the HK algorithm. Here $\omega_1 = 1.0$, $\theta(r_0) = 0.6$, $A_1 = -0.181463, B_1 = -1.01382$, $SNR = 0dB$.

		Cosine filter	Cos-bin filter
k	M_k	$\hat{\gamma}_{r_k}$	$\hat{\gamma}_{r_k}$
0	5	0.89580	1.04667
1	10	0.99953	1.04039
2	15	0.99953	1.03096
3	20	1.00110	1.01210
4	25	1.00110	1.00581
5	30	1.00110	1.00424
		$\hat{\omega}_1 = 1.00110$	$\hat{\omega}_1 = 1.00424$

5 Summary

Our observation is that for sufficiently long data records (e.g. $N \geq 1000$), and for a reasonable signal to noise ratio (e.g. $SNR \geq 0$), the original CM algorithm, as given in HK in terms of HOC from zero-crossings, performs remarkably well when the method employs bandpass filters. Furthermore, the method requires $O(N)$ computational complexity, compared with $O(N \log N)$ complexity associated with FFT based methods. In almost all the cases considered in the above examples, the HK algorithm outperformed the periodogram. This has been the case with numerous other examples, using a variety of filters. However, combining both methods may result in the improvement of both.

We emphasized the single frequency case. However, an extension to the multiple frequency case is rather straightforward because the CM method, when employing bandpass filters, can be applied independently to nonoverlapping frequency bands as done in KY. That this is indeed feasible was already seen in Example 3. As such, this scheme is ideal for parallel processing.

We have used only a few filters in connection with the CM method, but of course many more are available. Results concerning different filters will be dealt with elsewhere.

There is one more thing. We have mentioned earlier that for a zero-mean stationary Gaussian process with a mixed spectrum, the observed zero-crossing rate is not necessarily consistent for its expectation. More precisely, in KS it is shown that if the spectrum contains two or more atoms (that is, two or more jumps in the spectral distribution function), then $\hat{\gamma}_r$ does not converge to a constant as $N \to \infty$. However, when the spectrum is a mixture of an atomic component with a single atom, and an absolutely continuous component (noise), $\hat{\gamma}_r$ is almost surely consistent provided *both* the sinusoidal component and the noise component have the exact same first order autocorrelation. *This, rather esoteric, case is precisely what the HK algorithm gives in the limit.* To see this, consider the process (3), and let

$$X_t \equiv A_1 \cos(\omega_1 t) + B_1 \sin(\omega_1 t)$$

Then

$$Z_t = X_t + \zeta_t$$

Let $\{\mathcal{L}_r\}$ satisfy (4). Then for $r = r^* = \cos(\omega_1)$, we have,

$$\mathcal{L}_{r^*}(Z)_t = \mathcal{L}_{r^*}(X)_t + \mathcal{L}_{r^*}(\zeta)_t$$

Because r^* is a fixed point of $\rho_1(r)$, $\mathcal{L}_{r^*}(X)_t$ and $\mathcal{L}_{r^*}(\zeta)_t$ have r^* as their first order autocorrelation, and so

$$\hat{\gamma}_{r^*} \to E(\gamma_{r^*}) = \omega_1$$

almost surely. This means that when the HK algorithm converges (bandpass filters or not), the limiting zero-crossing rate is almost surly a constant.

Acknowledgement. The authors are grateful to Eric Slud for helpful comments.

Figures

Figure 1. (a). An attracting fixed point that practically coincides with $\cos(0.8)$ in $\rho_1(r, 20)$, $\omega_1 = 0.8$, $M = 20$, from the complex exponential filter. The derivative of $\rho_1(\alpha, 20)$ in a neighborhood of $\cos(0.8)$ is very close to 0. (b). The squared gain (14) with $M = 20$, and centered at $\theta = 0.8$.

Figure 2. (a). An attracting fixed point that practically coincides with $\cos(0.8)$ in $\rho_1(\alpha, 100)$, $\omega_1 = 0.8$, $M = 100$, from the complex filter in HK. The derivative of $\rho_1(\alpha, 100)$ in a neighborhood of $\cos(0.8)$ is close to 0. (b). The normalized squared gain (20) with $M = 100$, and centered at $\theta = 0.8$.

Figure 3. The squared gain of the cosine filter centered at $\theta = 1$, with $M = 20$, and centered at $\theta = 1.1$ with $M = 40$.

Figure 4. GATE I data: interpolated hourly rain rate averaged over a 280×280 km^2 area in the eastern Atlantic. $N = 450$.

REFERENCES

1. Barnett, J. and B. Kedem, " Zero-crossing rates of functions of Gaussian processes," To appear in *IEEE Trans. Infor. Th.*, July, 1991.

2. He, S. and B. Kedem, "Higher order crossings of an almost periodic random sequence in noise," *IEEE Trans. Infor. Th.*, 35, pp. 360-370, March 1989.

3. Kedem, B. and S. Lopes, "Fixed points in mixed spectrum analysis," *Probabilistic and Stochastic Methods in Analysis, With Applications*, NATO ASI, July 14-27, 1991, Il Ciocco, Italy.

4. Kedem, B. and E. Slud, "On Autocorrelation Estimation in Mixed-Spectrum Gaussian Processes," Submitted.

5. Kedem, B. and S. Yakowitz, "A contribution to Frequency Detection," submitted, 1990.

6. Simpson, J., *TRMM, A Satellite Mission to Measure Tropical Rainfall*, Report of the Science Steering Group, National Aeronautics and Space Administration, August, 1988.

7. Yakowitz, S. "Some contributions to a frequency location method due to He and Kedem," To appear in *IEEE Trans. Infor. Th.*, July, 1991.

Figure 1. (a). An attracting fixed point that practically coincides with $\cos(0.8)$ in $\rho_1(r, 20)$, $\omega_1 = 0.8$, $M = 20$, from the complex exponential filter. The derivative of $\rho_1(\alpha, 20)$ in a neighborhood of $\cos(0.8)$ is very close to 0. (b). The squared gain (14) with $M = 20$, and centerd at $\theta = 0.8$.

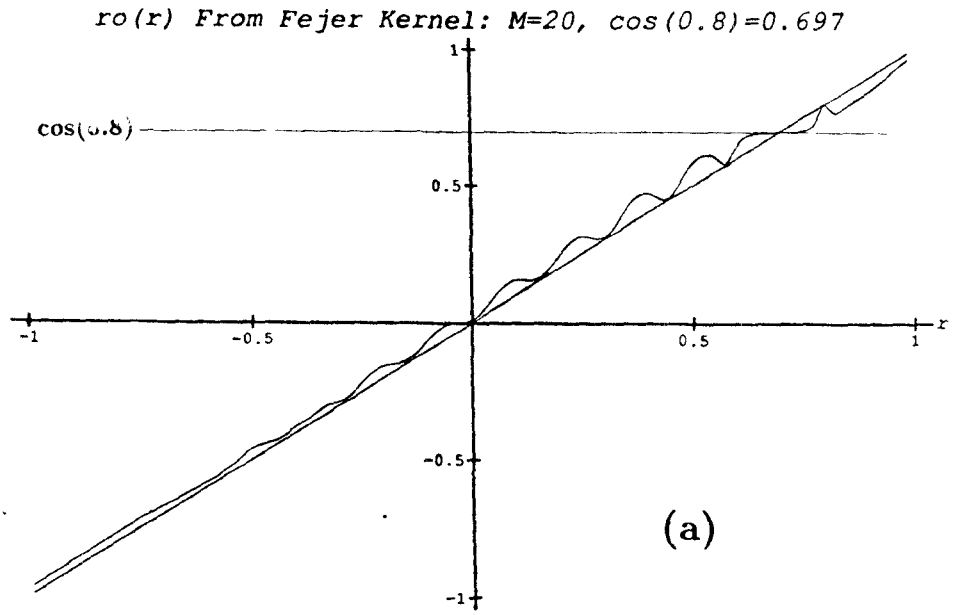

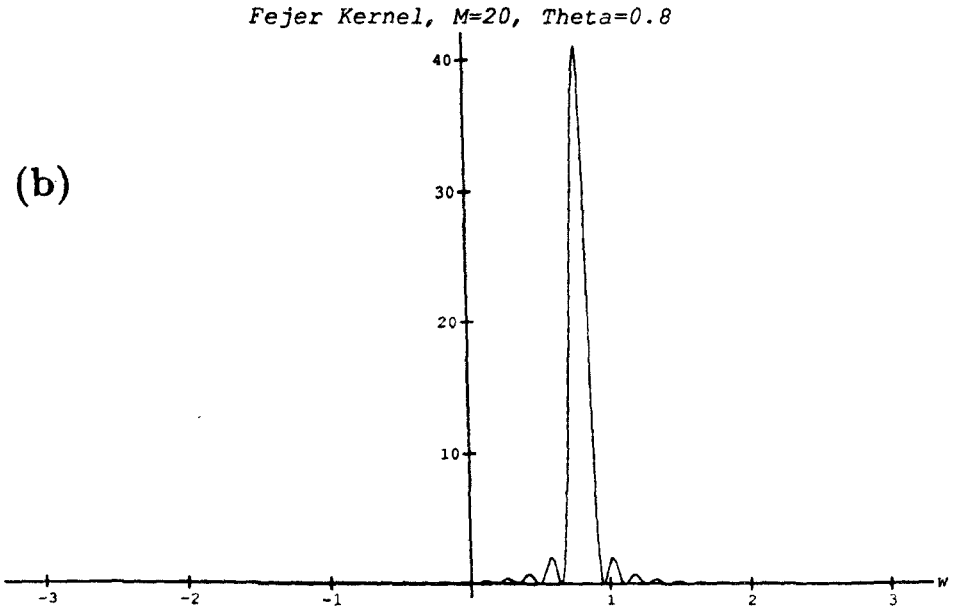

Figure 2. (a). An attracting fixed point that practically coincides with $\cos(0.8)$ in $\rho_1(\alpha, 100)$, $\omega_1 = 0.8$, $M = 100$, from the complex filter in HK. The derivative of $\rho_1(\alpha, 100)$ in a neighborhood of $\cos(0.8)$ is close to 0. (b). The normalized squared gain (20) with $M = 100$, and centerd at $\theta = 0.8$.

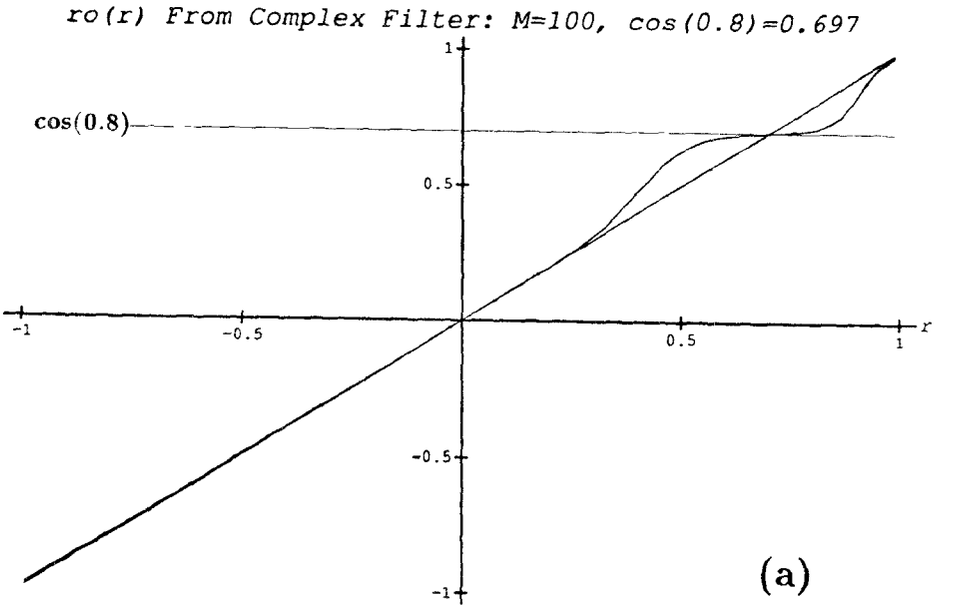

(a)

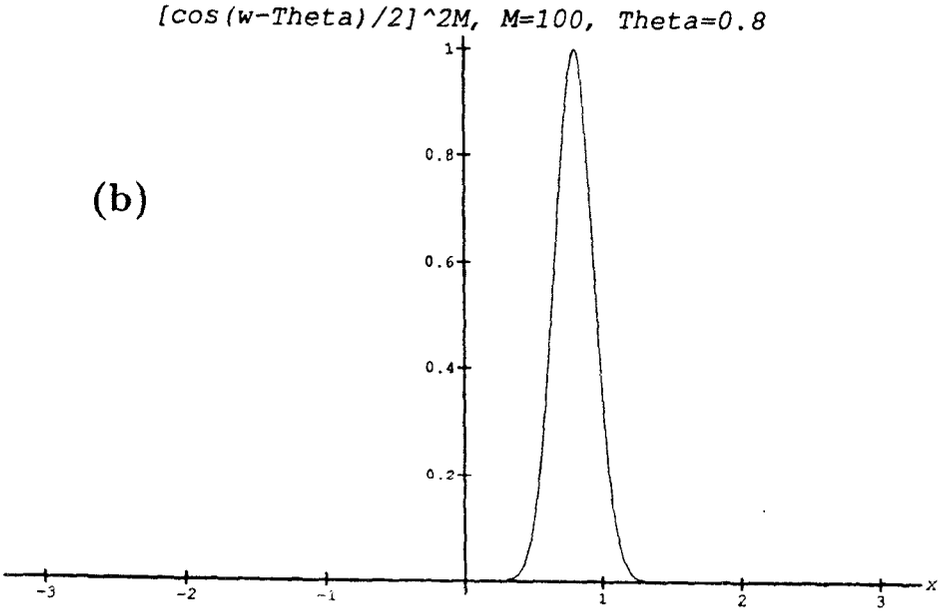

(b)

Figure 3. The squared gain of the cosine filter centered at $\theta = 1$, with $M = 20$, and centered at $\theta = 1.1$ with $M = 40$.

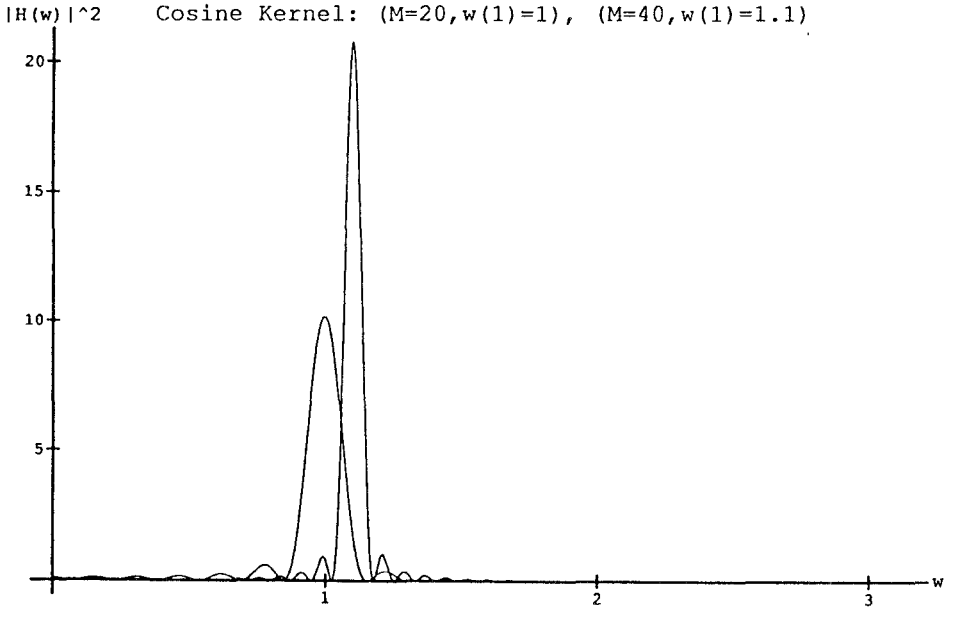

Figure 4. GATE I data: interpolated hourly rain rate averaged over a 280×280 km^2 area in the eastern Atlantic. $N = 450$.